Building Tomorrow's Society
Bâtir la Société de Demain

Fredericton, Canada
June 13 – June 16, 2018/ *Juin 13 – Juin 16, 2018*

FIBREGLASS SANDWICH BEAMS WITH 3D WOVEN FABRIC CORES

McCracken, Aidan[1], and Sadeghian, Pedram[1,2]
[1] Department of Civil and Resource Engineering, Dalhousie University, Canada
[2] Pedram.Sadeghian@dal.ca

Abstract: Composite sandwich beams composed of fibre-reinforced polymer (FRP) skins and low-density core materials have been shown to be effective in reducing weight and increasing structural efficiency in a variety of applications. The FRP skins resist the tensile and compressive stresses as a result of bending, while the core resists shear stresses, provides insulation and increases the distance between skins resulting in an increased moment of inertia. In this study, sandwich beams made of glass FRP (GFRP) skins and a 3D woven fabric is used for core are tested and analyzed. Specifically, either zero, one or two layers of fibreglass fabric were used for the skins and a 3D fabric, with a nominal thickness of 8 mm was used for the core. A total of 30 small-scale sandwich beam specimens were manufactured across six unique beam varieties with dimensions of 50 mm in width, 25 mm in depth, and 200 and 350 mm in length (150 mm and 300 mm spans) to be tested under four-point bending up to failure. The load-deflection behaviour of the test specimens was analyzed. Additionally, the flexural and shear stiffness of the sandwich specimens were calculated. Overall, the 3D fabric core displayed promising structural behaviour. However, it will be shown that as a result of the higher strength/stiffness skins, the sandwich beams with two layers of GFRP skin displayed weaker structural performance caused by a premature failure due to longitudinal shear stress. Thus, it may be concluded that compatibility between the skin and core is a key factor in optimizing composite sandwich beam performance.

1 INTRODUCTION

The abundance and usage of structural sandwich panels is increasing as engineers look to maximize the efficiency of many structural components. Typical sandwich panels consist of two thin, high-strength facesheets to resist tensile and compressive stresses of bending as well as a low-strength and low-density core material. Sandwich panels are often favoured in high-performance structural applications due to their relatively light weight and high moment of inertia (Reis and Rizkalla 2008). The use of a variety of fibre-reinforced polymer (FRP) skin materials have been studied such as fibreglass and carbon (Roberts et al. 2002, Fan et al. 2007, and Fam et al. 2016) as well as natural fibres such as flax (Sadeghian et al. 2016). In addition to separating the two facesheets to provide an increased moment of inertia, the core provides strength to resist transverse and longitudinal shear stresses and may also provide greatly improved thermal insulation (Allen 1969).

Many different core materials have been explored for use in composite sandwich beams and panels. Core materials that are commonly studied and implemented include low-density foam and plastic or metal honeycombs (Gupta and Woldesenbet 2005, Wadley et al. 2003). Three-dimensional (3D) woven fabrics have more recently been introduced and provide a viable alternative in sandwich construction (Bannister et al. 1999, Chou et al. 1992). 3D woven fabrics are manufactured multi-layered warp fibres in the structured direction, and two orthogonal sets of weft fibres which interlace with the warp fibres to provide structural stability in all directions (Khokar 2002). Although studies have previously been conducted on the structural performance of sandwich composites manufactured with a 3D fabric core, there is a multitude of woven

fabric styles. The core is often what governs failure in sandwich composites (Betts et al. 2018). Consequently, various styles of multi-dimensional cores must be studied to enhance strength and predictability surrounding sandwich composites manufactured with a 3D woven fabric core.

As compared to materials such as foam and honeycomb, a 3D fabric core may provide many significant manufacturing advantages. As the material is provided as a fabric, it is initially very flexible and can be used easily as a core in non-conventional applications such as curved surfaces and sandwich pipes. Whereas plastic or metal cellular cores may need to be cut to accommodate smaller radii, a fabric can simply be rolled into place before the curing process. Furthermore, as the FRP skins and core are cured at the same time, they will ideally have an improved structural unity and this may eliminate the risk of delamination, which is a common issue in sandwich panel construction (Chen 2002). Moreover, since the 3D fabric comes in a roll, it is a very easy to transport material and long lengths of composite beams can be produced without any seams or overlap in the core.

In this paper, glass FRP (GFRP) facesheets are combined with a 3D woven fabric core to manufacture sandwich beams with zero, one and two layers of GFRP skins. In the manufacturing of these panels, both the facesheets and core were cured using the same epoxy resin at the time. The aim of the study is to analyze and evaluate the structural performance of sandwich beams consisting of GFRP skins in combination with a singular style of 3D fabric core. Based on existing information, it can be concluded that 3D fabric holds great potential in the world of sandwich composites. As new fabrics are manufactured exclusively for structural purposes, their structural performance must be evaluated. In this study, multiple small-scale sandwich beams were manufactured and tested under four-point bending. Structural properties such as strength and stiffness as well as core properties such as shear modulus are evaluated. Moreover, the interaction between the GFRP skins and the 3D fabric core is analyzed.

2 EXPERIMENTAL PROGRAM

2.1 Test Matrix

A total of 30 sandwich specimens were fabricated to be tested under four-point bending. The variables were the number of layers of facing as well as the specimen span. Two different span lengths, 150 mm and 300 mm were tested. All specimens had an 8-mm nominal thickness 3D fabric core and had either 0, 1, or 2 layers of glass fibre-reinforced polymer (GFRP) skin. The test matrix is shown in Table 1. Five identical specimens were made for each case. The test specimens are identified with a specimen ID such as GX-SY where G stands GFRP, S stands for span, X identifies the number of GFRP skin layers and Y identifies the span length in mm. For example, G0-S150 is a 3D-fabric core sandwich beam with zero (0) layers of GFRP skin tested with a 150-mm span.

Table 1: Test matrix

Case #	Specimen ID	Number of skin layers	Span (mm)	Number of specimens
1	G0-S150	0	150	5
2	G0-S300	0	300	5
3	G1-S150	1	150	5
4	G1-S300	1	300	5
5	G2-S150	2	150	5
6	G2-S300	2	300	5
Total				30

2.2 Material Properties

For the GFRP skins, a 915 g/m^2 (gsm) unidirectional fibreglass fabric was used. The fabric was made of glass fibres with a density of 2.55 g/cm^2, a tensile strength of 3.24 GPa, an elastic modulus of 72.4 GPa and a rupture strain (ultimate elongation) of 4.5% all as reported by the manufacturer for the dry fibres. Five

identical GFRP tensile coupons made of two layers of the unidirectional fabric and epoxy resin were prepared using wet hand lay-up method and tested according to ASTM D3039 (2014). Figure 1 shows the tensile test results based on the nominal ply thicknesses of 1.3 mm as reported by the manufacturer. The average tensile strength of the GFRP coupons was 582.93 MPa with a standard deviation of 30.63. As shown in Figure 1, the GFRP coupons displayed a nearly linear behaviour up to the point of rupture. The average modulus of the GFRP coupons was 21.75 GPa with a standard deviation of 0.58.

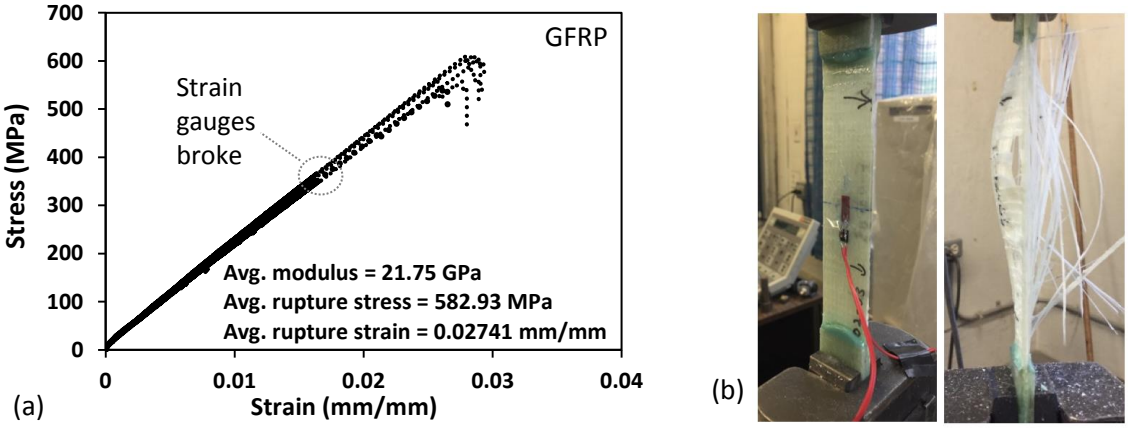

Figure 1: GFRP coupon tests: (a) stress-strain curves; and (b) coupon before and after testing.

Using the nominal aerial weight of 915 gsm (1830 gsm for two layers of fibreglass), the fibre weight fraction (FWF) of the GFRP coupons was calculated. The coupons had an average FWF of 0.52 (thus, 52% of the mass is contributed by fibres). Using Eq. (1), the fibre volume fraction (FVF) is calculated using the FWF, the density of the dry fibreglass (ρ_f) and the density of the matrix (ρ_m). The density of the dry fibreglass was reported to be 2.55 g/cm^3 and the solid matrix density was calculated to be 1.13 g/cm^3 as explained previously. The average FVF of the coupons was calculated as 0.327.

[1] $$\mathrm{FVF} = \frac{1}{1+\frac{\rho_f}{\rho_m}\left(\frac{1}{\mathrm{FWF}}-1\right)}$$

For the core of the sandwich specimens, a three-dimensional (3D) woven fabric was used. The fabric comes in a flexible roll and when cured with the epoxy resin it rises and stiffens into its full thickness. The nominal thickness after curing as reported by the manufacturer is 8 mm. Across 9 samples, an actual average thickness was found to be 7.54 mm after curing. Figure 2 (c) shows a cross-sectional view of a cured sample of 3D fabric. Note that after curing, the fabric core remains hollow as the resin does not clog any of the cells. The dry fabric was measured to have a weight of approximately 1050 gsm. When cured with the resin, the 3D fabric composite was measured to have an average weight of 2988 gsm with a standard deviation of 134.0. Accordingly, the 3D fabric composite specimens had an average FWF of 0.352.

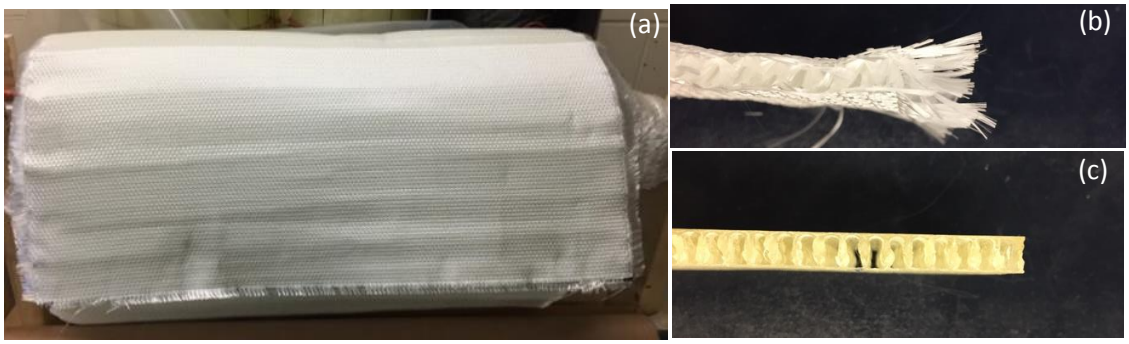

Figure 2: 3D core: (a) dry fabric roll; (b) dry fabric layer; and (c) cured with resin.

2.3 Specimen Fabrication

When producing the sandwich specimens, sheets of both fibreglass and 3D fabric (approximately 400 mm x 635 mm) were carefully cut using shears. Originally creating large panels allowed for a greater quantity of specimens to be manufactured at once. All specimens were fabricated using the wet lay-up method. Brushes and a roller were used to distribute the resin across the surface of the fabric and a spatula was used to smooth the layer of resin. In order to ensure that the 3D fabric core had enough resin, both sides of the fabric sheet were pre-saturated before applying it to the surface of the already saturated fibreglass skin. The specimens were prepared on a layer of parchment paper. Furthermore, an additional layer of parchment paper was applied to the top surface of the specimens as they cured for approximately 48 hours at room temperature. Parchment paper allowed the outer surfaces of the specimens to have a smooth and consistent finish. This style of production provided one large panel of the composite, which was then cut into the sandwich beams using a diamond-bladed miter saw after the curing process was complete. The composite panels were first cut into 50 mm wide strips. This was followed by them cutting them into either 200 mm or 350 mm long beams. An overhang length of 25 mm was considered at each support of the beam specimens. Thus, 200 mm and 350 mm long specimens had an actual span of 150 mm and 300 mm, respectively. A digital caliper was used to measure the width and thickness of each specimen at three locations and was averaged for further calculations. Fabricated specimens are shown in Figure 3.

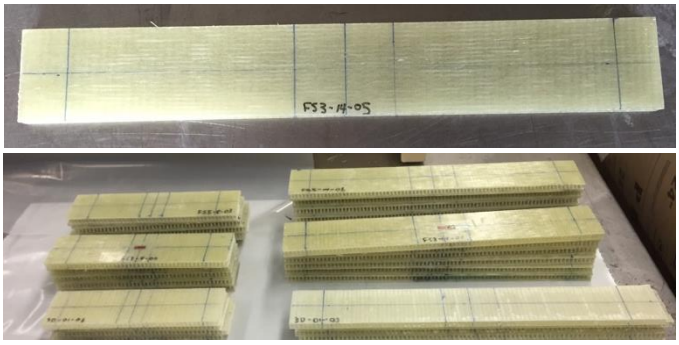

Figure 3: Fabricated specimens.

2.4 Test Setup and Instrumentation

For the sandwich beam testing, a four-point bending setup was used for all specimens with a different loading span proportional to the supporting span as shown in Figure 4. The loading span (L) was equal to (2/11) of the supporting span (S) per ASTM D7249 (2012) and ASTM D7250 (2012).

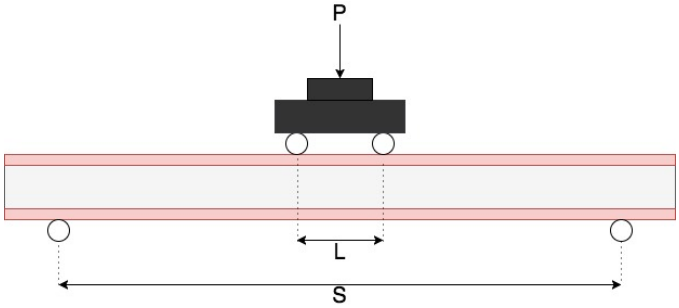

Figure 4: Four-point bending test setup (S=150 mm and S=300 mm).

In terms of instrumentation, each specimen had two strain gauges applied on the top and bottom in the longitudinal direction to measure the compressional and tensile strains, respectively. Additionally, two linear potentiometers (LPs) were placed directly in the middle of the span to measure the average mid-span deflection of the beams. Due to the size of the testing machinery, the LPs were not able to fit directly underneath the beams. Consequently, a thin and rigid piece of steel was secured to the bottom of the beams to keep contact with the top of the LPs; this steel did not affect the response of the beam and moved

downward along with the bottom of the beam. All tests were done with a 100 kN universal testing machine and were displacement controlled with a fixed rate of 2 mm/min.

3 RESULTS AND DISCUSSION

A summary of the test results as well as the mode of failure for each case is shown in Table 2. As previously mentioned, five specimens were tested per case, which had four specimens tested.

Table 2: Summary of test results

Specimen ID	Peak Load (N)		Initial Stiffness (N/mm)		Deflection at peak load (mm)		Failure Mode
	AVG	SD	AVG	SD	AVG	SD	
G0-S150	221.9	53.0	52.75	0.72	4.45	1.01	Core crushing
G0-S300	215.8	54.7	8.02	0.86	28.66	6.66	Core crushing
G1-S150	1424.6	312.8	230.06	57.87	21.10	5.54	Transverse shear
G1-S300	1323.9	148.1	71.06	6.97	34.92	3.14	Transverse shear
G2-S150	1572.9	90.0	182.92	10.06	31.45	4.17	Longitudinal shear
G2-S300	628.3	39.6	49.85	3.76	33.67	1.30	Longitudinal shear

Note: AVG = Average; SD = Standard deviation

As seen in Table 2, there were three different modes of failure observed during testing. The three modes of failure were crushing of the core facing (G0 specimens), core transverse shear failure (G1 specimens), and core longitudinal shear failure (G2 specimens). Although the zero, one- and two-layer specimens were controlled by a different mode of failure, it was the core that failed first each time. Thus, regardless of the facesheet thickness or strength, the core material is what limits the strength of these composite sandwich beams. As discussed, this behaviour is expected in sandwich composites. In the specimens with one and two layers of GFRP skin, no indentation, buckling or tensile rupture of the skins were observed. All three modes of failure can be seen in Figure 5.

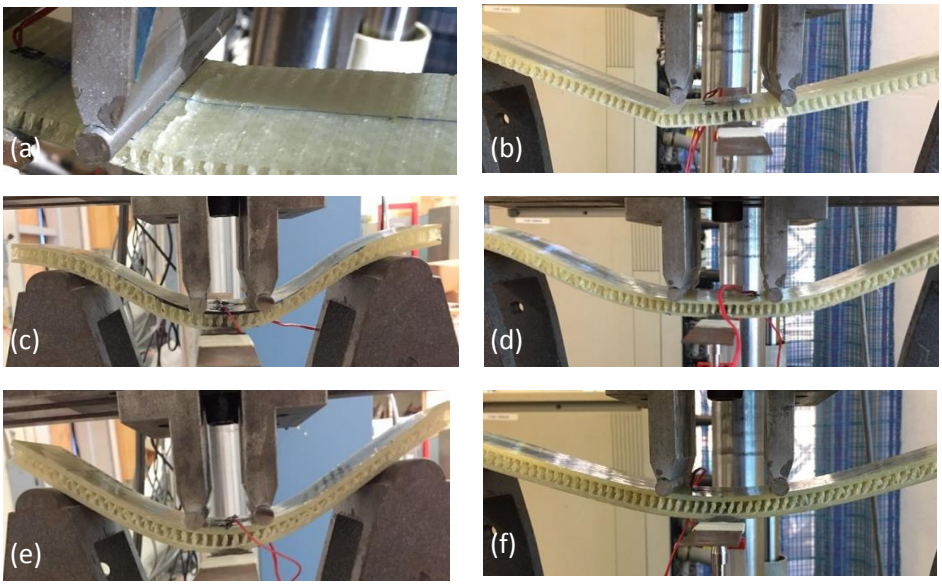

Figure 5: Modes of failure: (a) G0-S150 core crushing; (b) G0-S300 core crushing; (c) G1-S150 transverse shear; (d) G1-S300 transverse shear; (e) G2-S150 longitudinal shear; and (f) G2-S300 longitudinal shear.

An interesting observation during testing was how the core seemed to behave differently with one layer of facing (G1 specimens) in comparison to two layers (G2 specimens). During the one-layer tests, the vertical fibres of the core remained almost vertical as the core deformed due to transverse shear. During the two-layer tests, the same vertical fibres were forced to tilt diagonally due to the dominant longitudinal shear. This difference can be seen in detail in Figure 6.

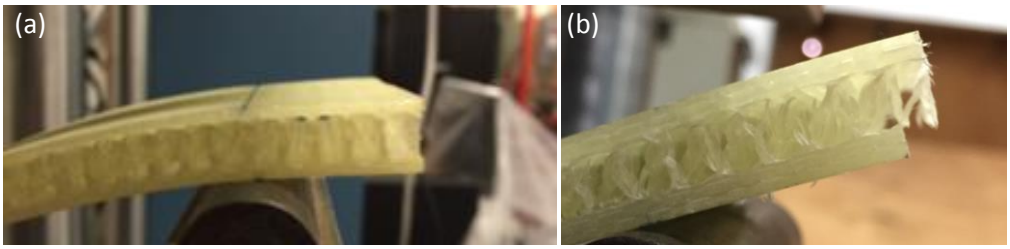

Figure 6: Core shear failure detail: (a) transverse; and (b) longitudinal.

It is hypothesized that the longitudinal core shear failure is due to significant partial composite behaviour of specimens with two-layer facing. This means that the core was not rigid enough to maintain a linear strain profile in the specimens with two-layer GFRP facings, which were twice as stiff compared to one-layer GFRP facings. The partial composite behaviour can be explained using the Timoshenko beam theory, rather than the common Euler-Bernoulli beam theory, and is discussed more in-depth in the following sections. The schematic shown in Figure 6 illustrates the main visual difference between the two theories. The Euler-Bernoulli theory assumes that the beams cross section remains perpendicular to the bending line while the Timoshenko theory allows for rotation due to shear deformation. When the shear deformation is small, Euler-Bernoulli theory approaches Timoshenko theory. In terms of sandwich beams, Euler-Bernoulli is an accurate model of the beam's behaviour when the core has adequate strength in both the transverse and longitudinal directions. Figure 7 shows the average load-deflection behaviour for the zero, one and two-layer sandwich beams. Figure 7(a) and 7(b) display the behaviour for the spans of 150 mm and 300 mm respectively.

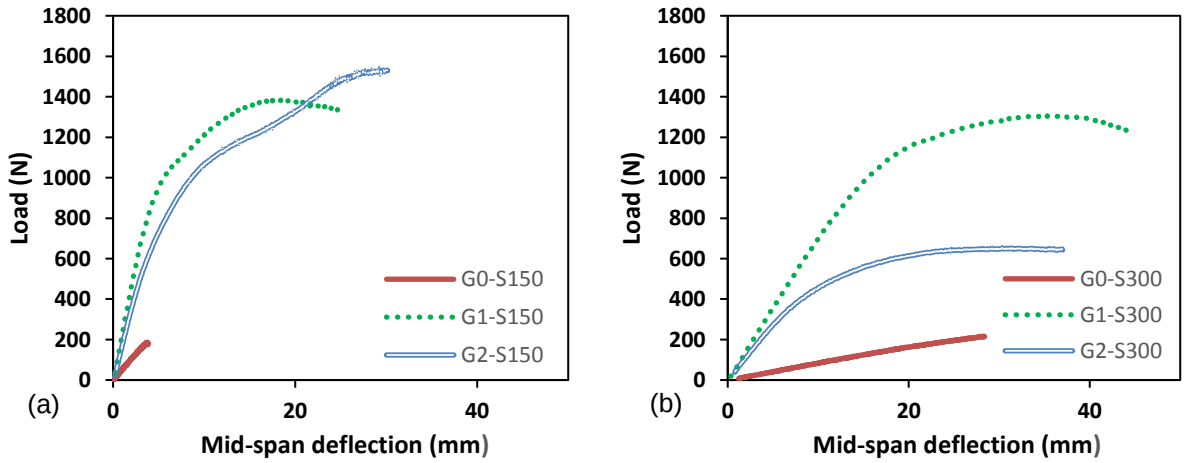

Figure 7: Average load-deflection diagrams: (a) 150 mm span; and (b) 300 mm span. (Note: each curve is the average of five identical specimens)

The zero-layer specimens displayed linear behaviour up to the point of instant failure due to crushing of the 3D core. The one and two-layer specimens displayed a section of linearity followed by a slowly ascending curve up to a peak load, as shown in Figure 7. As expected, the initial stiffness and peak load for both span lengths of the beams with zero layers of GFRP facesheets was substantially less than the one- and two-layer specimens. However, it is notable that the one-layer beams displayed a higher initial stiffness for both span lengths. This is theorized to be caused by the partial-composite behaviour by the two-layer specimens.

Since the strength of the facesheets is much higher than the strength of the core, the facesheets begin to behave independently. Thus, due to bending, the two facesheets begin to shift longitudinally with respect to each other, developing a longitudinal shear stress in the core. As the facesheet thickness increases, the longitudinal stiffness of the facesheet increases. This increases the normal stress in the facesheet and subsequently increases the longitudinal shear stress in the core. As the core is softer and weaker in the longitudinal direction compared to the vertical direction, the longitudinal shear deformation of the core governs the behaviour of the two-layer specimens. Accordingly, this weakness in the longitudinal direction of the core coupled with the increase in longitudinal shear stress may explain in the relative weakness of the two-layer specimens. This behaviour can be explained using the Timoshenko beam theory where plane sections do not remain plane throughout bending. Figure 8 shows the average load-deflection behaviour for the zero, one and two-layer sandwich beams. Figure 8(a) and 8(b) display the behaviour for the spans of 150 mm and 300 mm respectively.

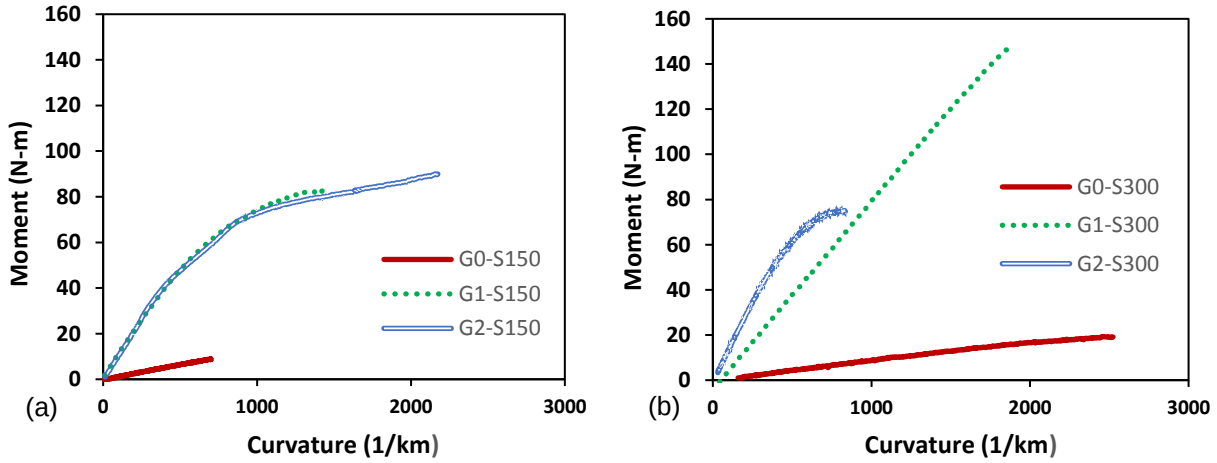

Figure 8: Average moment-curvature diagrams: (a) 150 mm span; and (b) 300 mm span. (Note: each curve is the average of five identical specimens)

As seen in Figure 8(a), the moment-curvature behaviour of the G1 and G2 specimens with a span of 150 mm was essentially identical. Thus, the flexural stiffness of the two beam types was the same, based on experimental calculations from the moment-curvature behaviour. Although the G2 specimens displayed a slightly higher flexural stiffness than the G1 specimens, they failed at much lower values of moment and curvature. This is again a result of the partial composite behaviour as the core failed due to longitudinal shear in the G2 specimens at a much lower load than the G1 specimens, which failed due to transverse shear. Although the lower load indicates a different failure mode, the lower than expected values for flexural stiffness of the G2 beams confirms that the partial composite behaviour affects the behaviour, regardless of the applied load.

The variability of test result for the specimens with two layers of GFRP was less than that of the specimens with one layer of GFRP. For example, the coefficient of variation of the peak load of the specimens with one and two layers of GFRP (span of 300 mm) were 10.71 and 6.30%. Also, the coefficient of variation (of the peak load of the specimens with one and two layers of GFRP (span of 150 mm) were 12.23 and 5.72%. Overall, the average coefficient of variation of the peak load of the specimens was 8.74%.

4 ANALYTICAL MODELLING

4.1 Flexural Stiffness and Transverse Shear Rigidity

Flexural stiffness (D) of the sandwich beams was calculated based on moment-curvature behaviour. Additionally, by using the experimental values of the initial stiffness of two span lengths, flexural stiffness (D) and transverse shear rigidity (U) can be calculated (Sadeghian et al. 2018) using Equation 2.

[2] $1 = K_1 \frac{(2S_1^3 - 3SL_1^2 + L_1^3)}{96D} + K_1 \frac{(S_1 - L_1)}{4U}$

where K is initial stiffness in N/mm, S is the span length in mm and L is the loading span in mm. Note that all occurrences of subscript i denotes that this is a value that is specific to each span length. For example, S1 represents the span length of 150 mm while S2 represents the span length of 300 mm. Using the experimental initial stiffness values for the 150 mm and 300 mm spans, values for D and U were calculated using Equation 2. Additionally, values for D were calculated by determining the initial slope of the moment vs. curvature curves which are shown in Figure 8. Table 3 displays both calculated values for flexural stiffness for G0, G1 and G2 sandwich beams as well as the calculated values for transverse shear rigidity.

4.2 Core Properties

An important property of the core, the shear modulus (G_c), can be calculated using Equation 3 where b is the width of the beam, t is the skin thickness, c is the core thickness, d is the thickness measured from the centre of each skin and h is the height of the entire composite sandwich beam. All dimensions have units of mm for further calculations.

[3] $G_c = \frac{U(h-2t)}{(h-t)^2 b}$

Table 3: Flexural and shear properties of sandwich beams

Group ID	Flexural stiffness, D (N-m^2)		Transverse shear rigidity, U (kN)
	Based on Equation 2	Based on Curvature	Based on Equation 2
G0	5.87	4.43	7.56
G1	54.76	74.76	10.84
G2	58.90	53.86	12.06

Figure 9(a) illustrates the variation in transverse shear rigidity between the G0, G1 and G2 specimens. Additionally, the average of these three values is displayed on the figure. It indicated that the transverse shear rigidity does not change with adding GFRP skins. Figure 9(b) displays the variation in core shear modulus for the G0, G1 and G2 specimens. The core shear modulus decreased slightly with each layer of GFRP skin added. The sandwich beams had an average core shear modulus of 16.60 MPa.

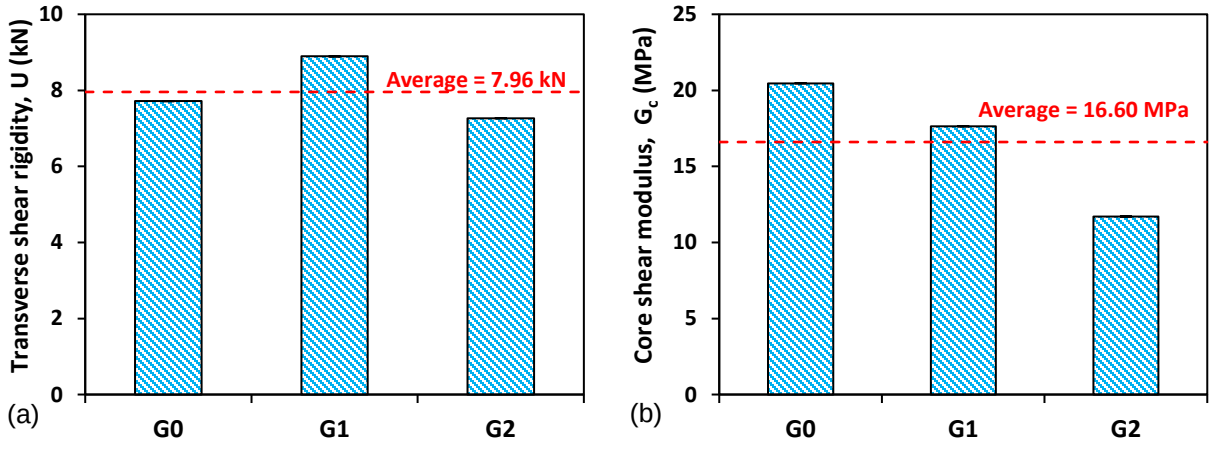

Figure 9: Variation in (a) transverse shear rigidity and (b) core shear modulus.

Sadeghian et al. (2018) had previously studied the properties of sandwich beams manufactured with GFRP facesheets and a polypropylene honeycomb core. Honeycomb thicknesses of 6 mm and 12 mm were

shown to have and average transverse shear rigidity of 6.2 kN and 9.2 kN and an average core shear modulus of 13.9 GPa and 11.8 GPa respectively. In this study, the 3D fabric core displayed an average transverse shear rigidity of 7.96 kN and an average core shear modulus of 16.60 GPa. The results indicate that the 3D fabric core used in this study had comparable and even higher shear rigidity and modulus properties. However, the number the number of GFRP skin layers should be limited to have ensure there is a compatibility between the skins and the core. More research with different 3D fabric cores is needed to characterize the behaviour of sandwich composted with 3D fabric cores.

5 CONCLUSION

In this study, small-scale sandwich beams manufactured with GFRP facesheets and a 3D fabric core were tested and analyzed. A total of 30 specimens were considered, with either zero, one or two facesheets and two span lengths of 150 mm and 300 mm. Overall, it may be concluded that this specific 8 mm 3D fabric is a viable option for the use in structural sandwich panels. The core displayed very similar, and sometimes slightly better, shear rigidity and modulus properties in comparison with a polypropylene honeycomb that had been previously studied. Additionally, as discussed, the 3D fabric may have many economic and logistical advantages compared to honeycomb materials, which are commonly used in sandwich panel construction. However, it must be noted that the number of layers of GFRP facesheets should be limited to one. Compatibility between the facesheet and core materials is crucial in sandwich beams, and this studied illustrated that adding a second layer of GFRP compromised the structural behaviour of the beams. Peak load and flexural rigidity values both decreased when a second layer was added to the facesheet. This is theorized to be caused by an increase in longitudinal stress in the core. Although the core is designed to have strength in the vertical direction, it was not able to resist the increased longitudinal stresses. As a result, the two facesheets began to behave independently and the cross section of the beam was no longer perpendicular to the bending axis. Overall, it can be seen that for this specific 3D fabric, one layer of facesheet is ideal for optimal structural performance. However, more studies must be conducted on various 3D fabrics to fully understand the behaviour of these fabrics as cores in sandwich beams and to make overarching recommendations in terms of design applications.

6 ACKNOWLEDGEMENTS

The authors of this paper would like to acknowledge the efforts of the technicians at Dalhousie University's Civil Engineering Department, Jesse Keane and Brian Kennedy, who helped immensely with the setup, instrumentation and testing process. In addition, the authors acknowledge the National Science and Engineering Research Council of Canada (NSERC) for the Undergraduate Student Research Award (USRA) for the first author, Dalhousie University for supplemental funding through the Innovation-Themed Undergraduate Research Funding, and QuakeWrap Inc. (Tucson, AZ, USA) for providing the fibreglass and 3D fabrics as well as the epoxy resin used in specimen fabrication.

7 REFERENCES

Allen, H.G., 1969. *Analysis and Design of Structural Sandwich Panels*. 1st ed., Pergamon Press, New York, NY, USA.

ASTM D3039. 2014. Standard Test Method for Tensile Properties of Polymer Matrix Composite Materials. American Society of Testing and Materials International, West Conshohocken, PA, USA.

ASTM D7249. 2012. Standard Test Method for Facing Properties of Sandwich Constructions by Long Beam Flexure. American Society of Testing and Materials International, West Conshohocken, PA, USA.

ASTM D7250. 2012. Standard Practice for Determining Sandwich Beam Flexural and Shear Stiffness. American Society of Testing and Materials International, West Conshohocken, PA, USA.

Bannister, M.K., Braemar, R., and Crothers, P.J., 1999. The Mechanical Performance of 3D Woven Sandwich Composites. Composite Structures. **47**(1-4), 687-690.

Betts D., Sadeghian P., and Fam A., 2018. Experimental Behavior and Design-Oriented Analysis of Sandwich Beams with Biobased Composite Facings and Foam Cores. *ASCE Journal of Composites for Construction*, **22**(4), 04018020.

Chen, J., 2002. Predicting Progressive Delamination of Stiffened Fibre-Composite Panel and Repaired Sandwich Panel by Decohesion Models. *Journal of Thermoplastic Composite Materials*. **15**(5), 429-442.

Chou S., Chen, H.C., and Wu, C.C., BMI resin composites reinforced with 3D carbon-fibre fabrics. *Composites Science and Technology*. **43**(2), 117-128.

Fam, A., Sharaf, T. and Sadeghian, P., 2016. Fiber element model of sandwich panels with soft cores and composite skins in bending considering large shear deformations and localized skin wrinkling. *Journal of Engineering Mechanics*, **142**(5), 04016015.

Fan H.L., Meng F.H., and Yang W., 2007. Sandwich Panels with Kagome Lattice Cores Reinforced by Carbon Fibers. *Composite Structures*. **81**(4), 533-539.

Gupta N., and Woldesenbet, E., Characterization of flexural properties of syntactic foam core sandwich composites and effect of density variation. *Journal of Composite Materials*. **39**(24), 2197-2212.

Khokar, N., inventor; Biteam AB, assignee. 2002. Woven 3D fabric material. United States patent US 6,338,367.

Reis, E.M., and Rizkalla, S.H., 2008. Material characteristics of 3-D FRP sandwich panels. *Construction and Building Materials*. **22**(6),1009-1018.

Roberts, J. C., Boyle, M.P., Wienhold, P.D., and White, G.J., 2002. Buckling, collapse and failure analysis of FRP sandwich panels. *Composites Part B: Engineering*. **33**(4), 315-324.

Sadeghian, P., Hristozov, D. and Wroblewski, L. 2018. Experimental and analytical behavior of sandwich composite beams: Comparison of natural and synthetic materials. *Journal of Sandwich Structures and Materials*, **20**(3), 287–307.

Wadley, H.N., Fleck, N.A. and Evans, A.G. 2003. Fabrication and structural performance of periodic cellular metal sandwich structures. *Composites Science and Technology*. **63**(16), 2331-2343.